# Clinical Applications and Controversies of Whole-Body MRI: *AJR* Expert Panel Narrative Review

Shivani Ahlawat, MD[1], Patrick Debs, MD[1], Behrang Amini, MD, PhD[2], Frédéric E. Lecouvet, MD, PhD[3], Patrick Omoumi, MD, MSc, PhD[4], Daniel E. Wessell, MD, PhD[5]

**Musculoskeletal Imaging · *AJR* Expert Panel Narrative Review**

**Keywords**

DWI, Li-Fraumeni syndrome, metastatic disease, multiple myeloma, pregnancy, whole-body MRI

Submitted: Jul 1, 2022
Revision requested: Jul 13, 2022
Revision received: Sep 12, 2022
Accepted: Sep 20, 2022
First published online: Sep 28, 2022
Version of record: Feb 1, 2023

S. Ahlawat received funding for research from Neurofibromatosis Therapeutic Acceleration Program and the U.S. Department of Defense. The remaining authors declare that there are no other disclosures relevant to the subject matter of this article.

Whole-body MRI (WB-MRI) is increasing in clinical acceptance and utilization for a range of indications. WB-MRI is currently an established screening tool for children and adults at high risk of developing malignancy, with the strongest supporting evidence in patients with Li-Fraumeni syndrome. WB-MRI has been added to professional society guidelines for staging disease in patients with certain malignancies including multiple myeloma and has been proposed as a technique to screen for metastatic disease in patients with visceral malignancies including prostate cancer and breast cancer. Emerging data support the utility of WB-MRI in children with malignancies such as Ewing sarcoma, in adults with myxoid liposarcoma, and in pregnant patients with occult or newly detected malignancy. WB-MRI can further help evaluate disease extent and treatment response in patients with nononcologic conditions such as chronic nonbacterial osteomyelitis, myopathy, inflammatory arthritis, and fever of unknown origin. This *AJR* Expert Panel Narrative Review summarizes available evidence and recommendations supporting the clinical applications of WB-MRI. This article also highlights limitations, barriers, and controversies associated with utilization of WB-MRI in routine clinical practice.

Whole-body MRI (WB-MRI) has been available for clinical use since the early 2000s and is increasing in clinical acceptance and utilization. As a result of technologic advancements, WB-MRI can now evaluate from the vertex to the knees or feet in a single session lasting 25–90 minutes, depending on the clinical indication. In comparison with the use of PET/CT for whole-body imaging, WB-MRI does not expose patients to ionizing radiation, providing an important benefit for children and young adults who require repeat examinations.

Among its applications (Table 1), WB-MRI is most commonly used for oncologic indications, with the two main such indications being screening for malignancy in high-risk patients (i.e., patients with genetic cancer predisposition syndromes such as Li-Fraumeni syndrome [LFS]) and staging or surveillance in patients with known malignancy. Emerging nononcologic indications for WB-MRI are also being explored, including multifocal aseptic musculoskeletal disorders (e.g., chronic nonbacterial osteomyelitis [CNO]); synovitis, acne, pustulosis, hyperostosis, and osteitis (SAPHO); congenital or acquired myopathy; inflammatory arthritis; and fever of unknown origin (FUO) [1–5].

This *AJR* Expert Panel Narrative Review has two primary purposes: to summarize the current evidence and recommendations on clinical applications of WB-MRI and to discuss controversies and barriers associated with incorporation of WB-MRI into clinical practice.

## Whole-Body MRI: Clinical Applications

### *Oncologic Applications*

Oncologic indications comprise the main clinical purpose for performing WB-MRI. In patients with genetic cancer predisposition syndromes, WB-MRI is performed as a screening tool for early detection of malignancy. The Oncologically Relevant Findings Reporting and Data System (ONCO-RADS) was developed to standardize the acquisition, interpreta-

ARRS is accredited by the Accreditation Council for Continuing Medical Education (ACCME) to provide continuing medical education activities for physicians.

The ARRS designates this journal-based CME activity for a maximum of 1.00 AMA PRA Category 1 Credit™. Physicians should claim only the credit commensurate with the extent of their participation in the activity.

To access the article for credit, follow the prompts associated with the online version of this article.

doi.org/10.2214/AJR.22.28229

*AJR* 2023; 220:463–475

ISSN-L 0361–803X/23/2204–463



[1]Russell H. Morgan Department of Radiology and Radiological Science, Johns Hopkins Medical Institutions, 601 N Caroline St, 3rd Fl, Baltimore, MD 21287. Address correspondence to S. Ahlawat (sahlawa1@jhmi.edu, @ahlawat_shivani).

[2]Department of Musculoskeletal Imaging, MD Anderson Cancer Center, Houston, TX.

[3]Department of Radiology, Institut de Recherche Expérimentale et Clinique (IREC), Cliniques Universitaires Saint Luc, Université Catholique de Louvain, Brussels, Belgium.

[4]Department of Diagnostic and Interventional Radiology, Lausanne University Hospital and University of Lausanne, Lausanne, Switzerland.

[5]Department of Radiology, Mayo Clinic, Jacksonville, FL.

**TABLE 1: Current Applications of Whole-Body MRI**

| Condition | Applications | Typical FOV |
|---|---|---|
| Oncologic applications | | |
| Genetic cancer predisposition syndromes | | |
| Li-Fraumeni syndrome | Screening for soft-tissue and/or bone sarcoma | Vertex to feet |
| NF1, NF2, schwannomatosis | Detection of internal tumor burden<br>Screening for MPNST | May extend from vertex to feet based on clinical need |
| Hereditary pheochromocytoma or paraganglioma syndromes | Screening for nonsecretory paraganglioma | Vertex to pelvis |
| Multiple hereditary exostoses and enchondromatoses | Detection of secondary chondrosarcoma | Vertex to feet |
| Known malignancies | | |
| Multiple myeloma | Staging of internal tumor burden<br>Assessment of treatment response | Vertex to knees |
| Lymphoma | Staging of indolent Hodgkin lymphoma and NHL | Vertex to knees |
| Solid primary cancer | Detection of skeletal, nodal, and visceral metastatic disease | Vertex to knees |
| Bone or soft-tissue sarcoma | Detection of skip metastases in osteosarcoma and Ewing sarcoma<br>Detection of soft-tissue and bone metastases in myxoid liposarcoma | Vertex to knees |
| Any malignancy detected in a pregnant patient | Detection of sites of unknown primary malignancy<br>Staging of cancer discovered during pregnancy | Vertex to knees |
| Nononcologic applications | | |
| Muscle disorders | | |
| Inflammatory myositis | Detection of disease extent (involvement of muscle groups and fasciitis)<br>Biopsy guidance<br>Assessment of treatment response | Vertex to feet |
| Congenital myopathy | Detection of disease extent and severity<br>Assessment of treatment response | Vertex to feet |
| Seronegative arthritis | | |
| Axial spondyloarthritis | Detection of inflammatory lesions including enthesitis<br>Assessment of treatment response | Vertex to feet |
| Psoriatic arthritis | Detection of inflammatory lesions including enthesitis<br>Assessment of treatment response | Vertex to feet |
| Other | | |
| Chronic nonbacterial osteomyelitis and/or chronic recurrent multifocal osteomyelitis | Detection of disease activity<br>Assessment of treatment response | Vertex to feet |
| SAPHO | Detection of disease activity<br>Assessment of treatment response | Vertex to feet |
| Fever of unknown origin | Detection of clinically occult site of infection or inflammation (especially in immunocompromised patients) | Vertex to feet |

Note—NF1 = neurofibromatosis 1; NF2 = neurofibromatosis 2; MPNST = malignant peripheral nerve sheath tumor; NHL = non-Hodgkin lymphoma; SAPHO = synovitis, acne, pustulosis, hyperostosis, and osteitis.

tion, and reporting of WB-MRI for cancer screening [6]. In patients with known malignancy, WB-MRI can evaluate disease extent, assess treatment response, and serve as a surveillance strategy for disease progression or recurrence [7].

### *Screening for Malignancy*

Among patients with genetic cancer predisposition syndromes, those with LFS are at particularly high risk, having a cumulative cancer risk of 90% by the age of 60 years [8]. In addition, due to radiation exposure, patients with LFS have a higher rate of secondary malignancy relative to the general population [9]. The spectrum of malignancies associated with LFS includes brain tumors, breast cancer, adrenocortical carcinoma, soft-tissue sarcoma, osteosarcoma, and leukemia. In patients with LFS, baseline WB-MRI yields a cancer detection rate of 7% [10]. Prospective multicenter data support annual screening WB-MRI as part of surveillance programs for patients with LFS, along with physical examination, laboratory testing, other imaging studies, and colonoscopy [11–13]. Among patients with LFS, those who undergo surveillance including WB-MRI have significantly improved 3-year survival compared with those who do not undergo surveillance [11]. Given the available data, the NCCN recommends

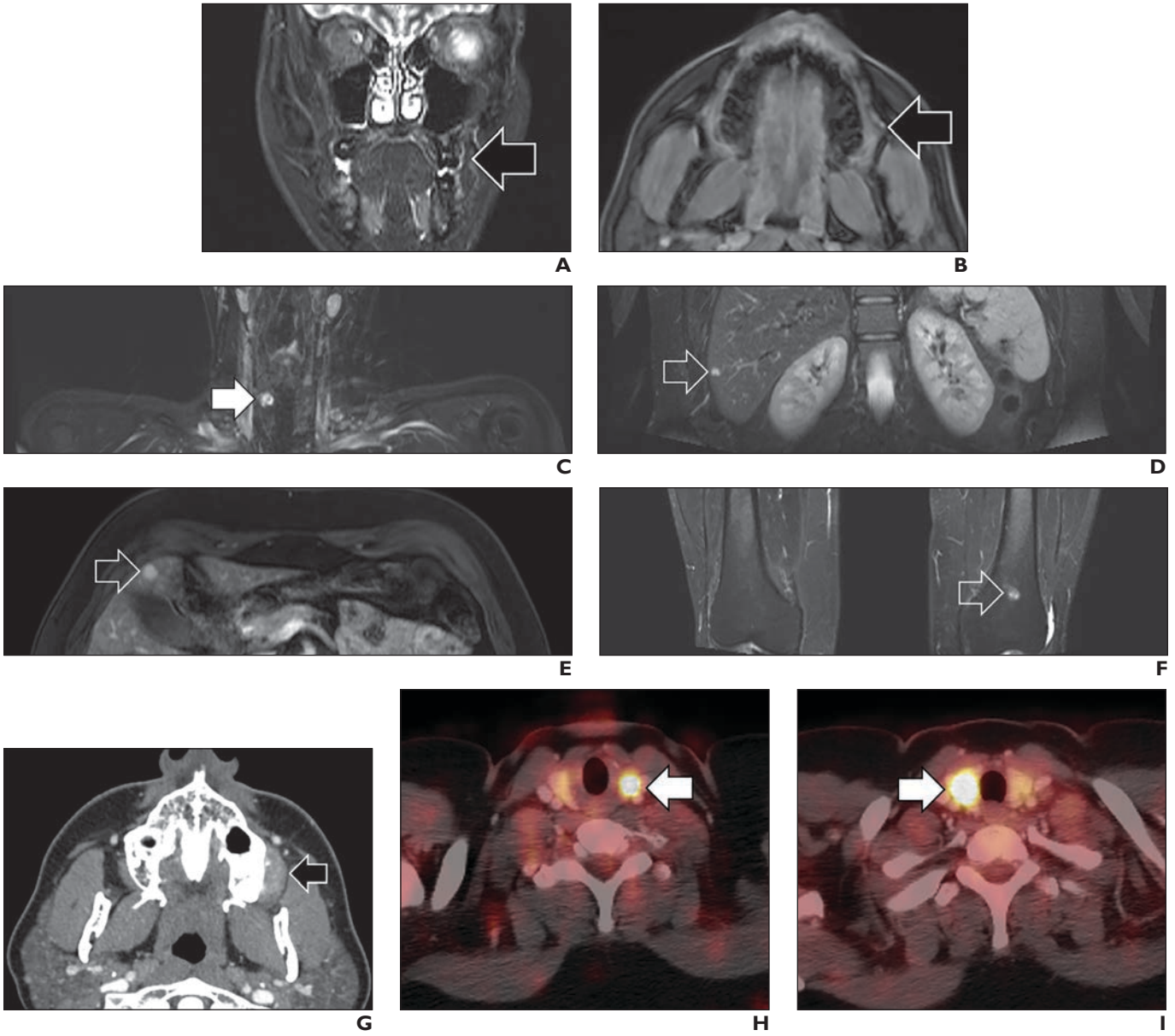


**Fig. 1—**35-year-old patient with Li-Fraumeni syndrome, no personal cancer history, and family history of pancreatic cancer and breast cancer.
**A** and **B,** Coronal STIR image (**A**) and axial postcontrast T1-weighted image with fat saturation (FS) (**B**) from baseline whole-body MRI (WB-MRI) show normal left maxilla (*arrow*).
**C,** Coronal STIR image from baseline WB-MRI shows thyroid nodules (*arrow*). Additional thyroid nodule was detected on baseline WB-MRI (not shown). Thyroid nodules were considered likely benign due to small size and multiplicity.
**D,** Coronal STIR image from baseline WB-MRI shows hepatic lesion (*arrow*), which had been characterized as cyst on previous abdominal MRI (not shown) performed due to family history of pancreatic cancer.
**E,** Axial postcontrast T1-weighted image with FS from baseline WB-MRI shows enhancing hepatic focus (*arrow*) that was characterized as perfusion-related phenomenon on previous abdominal MRI (not shown).
**F,** Coronal STIR image from baseline WB-MRI shows lesion (*arrow*) in distal left femur that was characterized as enchondroma on conventional radiography (not shown). Patient's insurance carrier declined coverage of 1-year follow-up WB-MRI examination. Patient developed palpable facial mass approximately 2 years after baseline WB-MRI.
**G,** Axial contrast-enhanced CT image obtained 2 years after baseline WB-MRI to assess facial mass shows soft-tissue mass (*arrow*) arising from left maxilla. Biopsy of mass showed osteosarcoma.
**H** and **I,** Serial axial fused FDG PET/CT images obtained for staging of osteosarcoma 2 years after baseline WB-MRI show FDG-avid lesions in thyroid gland (*arrows*). Biopsy revealed bilateral papillary thyroid carcinomas. Patient underwent treatment, including cytotoxic chemotherapy, for these malignancies. Patient developed therapy-related myelodysplastic syndrome (MDS) 3 years later and died 1 year after diagnosis of MDS. This case shows challenges of incidental findings, interval cancers, and reimbursement when performing WB-MRI.

that patients with LFS undergo annual screening for the early detection of malignancy that includes WB-MRI in addition to dedicated brain MRI, breast MRI or mammography, abdominal ultrasound, colonoscopy and esophagogastroduodenoscopy, and serum laboratory testing [14] (Fig. 1).

Limited data support the use of WB-MRI as a screening tool for patients with genetic cancer predisposition syndromes other than LFS, such as peripheral nerve tumor syndromes (neurofibromatosis type 1 [NF1], neurofibromatosis type 2 [NF2], schwannomatosis), hereditary pheochromocytoma or paraganglioma syn-

dromes, and multiple hereditary exostoses and enchondromas. The Response Evaluation in Neurofibromatosis and Schwannomatosis (REiNS) international collaboration recommends performing WB-MRI in patients with NF1 as a screening tool for the detection of internal plexiform neurofibromas, which can be a risk factor for the future development of malignant peripheral nerve sheath tumor (MPNST) [15]. The use of WB-MRI in these patients is supported by single-institution retrospective data showing higher internal plexiform tumor burden in patients younger than 30 years with NF1 and MPNST compared with age- and sex-matched patients with NF1 without MPNST [16]. In patients with hereditary pheochromocytoma or paraganglioma syndromes, a truncated WB-MRI protocol that evaluates from the vertex through the pelvis is recommended for the early detection of asymptomatic (i.e., nonsecretory) paragangliomas [17]. In a study of 37 patients with hereditary pheochromocytoma or paraganglioma syndrome and known or suspected succinate dehydrogenase (*SDH*) gene mutation, WB-MRI detected six paragangliomas (five asymptomatic), with higher sensitivity (87.5% vs 37.5%) and similar specificity (94.7% vs 94.9%) relative to laboratory testing [18]. An additional single-center retrospective study of 62 patients with multiple hereditary exostoses and enchondromatosis showed that a screening strategy including WB-MRI could detect asymptomatic secondary chondrosarcomas [19].

In summary, the strongest evidence supporting the added value of WB-MRI screening is found in LFS, and WB-MRI is included as a screening tool in the management of patients with this cancer predisposition syndrome. Interest is also emerging in the use of WB-MRI as a screening tool for the early detection of NF1-related MPNST; although expert recommendations for NF1 include WB-MRI, further prospective investigation is necessary.

### *Staging for Malignancy*

Imaging has a central role in patients with multiple myeloma (MM) according to the revised International Myeloma Working Group (IMWG) diagnostic criteria, which defines a lesion size on MRI of 5 mm as a threshold for defining an unequivocal active lesion [20, 21]. Prospective observational data show that WB-MRI can detect a greater number of myeloma lesions in comparison with FDG PET/CT [22]. WB-MRI has therefore been incorporated into the IMWG recommendations for MM. An *AJR* Expert Panel Narrative Review from 2021 [23] highlighted the role of WB-MRI in the diagnosis and management of patients with monoclonal gammopathy of undetermined significance (MGUS), solitary plasmacytoma, smoldering myeloma, and MM. For initial staging workup of patients with suspected MGUS, smoldering myeloma, and suspected MM, the IMWG recommends performing WB-MRI in the setting of inconclusive or negative low-dose whole-body CT or FDG PET/CT. In patients with solitary plasmacytoma, WB-MRI is recommended for the detection of diffuse or focal marrow infiltration, which may be occult on other imaging tests. MRI has high sensitivity for the early detection of bone marrow disease, which can improve clinical outcomes, whereas CT detects lesions at later stages when osteolysis is present [20, 21]. WB-MRI can also be performed for surveillance and assessment of treatment response. The Myeloma Response Assessment and Diagnosis System (MY-RADS) provides robust guidance for the use of WB-MRI in MM, as well as recommendations for acquisition, interpretation, and reporting, to optimize clinical care and clinical trials [20, 21]. WB-MRI, when available, should be considered the first-line diagnostic tool for the clinical management of patients with MM, including initial workup, staging, response evaluation, and surveillance; whole-body CT may be selected instead on the basis of local availability.

WB-MRI has also been investigated in patients with lymphoma, skeletal metastases from visceral malignancy, and soft-tissue and skeletal metastases from myxoid liposarcoma (MLS). In a meta-analysis of eight studies including 338 patients with Hodgkin lymphoma or aggressive non-Hodgkin lymphoma (NHL), WB-MRI and FDG PET/CT achieved similar diagnostic accuracy (98% and 98%) [24]. However, WB-MRI achieved higher diagnostic accuracy for lesion detection relative to FDG PET/CT when assessing indolent (i.e., non–FDG-avid) Hodgkin lymphoma (96% vs 87%, respectively) and NHL (98% vs 60%) [24].

In a large meta-analysis of patients with lymphoma, MM, and sarcoma, WB-MRI with DWI had higher sensitivity than WB-MRI without DWI (94% vs 55%, respectively) for treatment response assessment [25]. WB-MRI with DWI and ADC maps enables both qualitative lesion detection and quantitative measurement of lesions' ADC value as a potential marker of cellularity and/or tumor viability. Comparison of ADC values between pre- and posttreatment WB-MRI can help identify residual viable neoplasm in patients who do not respond to a particular treatment paradigm [25, 26]. A modified Dixon chemical-shift sequence also enables quantitative analysis through fat quantification, which can help differentiate marrow replacement from non–marrow replacement as well as help determine therapeutic response [27]. Specifically, in patients with MM, fat fraction (FF) analysis can help differentiate diffuse marrow infiltration due to MM (lower FF) from hematopoietic or normal bone marrow (higher FF) [28]. Nonetheless, prior studies have provided conflicting results regarding the performance of FF for such purposes, and the differentiation is particularly challenging in patients with superimposed hyperplastic hematopoietic marrow or anemia [29, 30].

WB-MRI has been evaluated for the detection of metastatic disease from visceral malignancies, including non–small cell lung cancer [31], testicular germ cell cancer [32], prostate cancer [33], rectal cancer [34], breast cancer [35], head and neck squamous cell carcinoma [36], gastric cancer [37], and melanoma [38]. WB-MRI can be particularly useful when a targeted PET radiotracer is unavailable (e.g., $^{68}$Ga-PSMA-11 for a patient with prostate cancer) or nonexistent (e.g., limited applicability of tracers including FDG for invasive lobular breast cancer) [39]. WB-MRI facilitates TNM classification for staging through simultaneous depiction of regional or distant lymphadenopathy, as well as visceral or bone metastases, although local assessment of the primary tumor usually requires a separate dedicated imaging examination [2] (Fig. 2).

Among visceral malignancies, WB-MRI has been most heavily investigated for evaluation of prostate cancer. Although PSMA PET/CT is the most sensitive method of detection and surveillance of metastatic disease in patients with prostate cancer, WB-MRI can play an important role in patients with advanced castration-resistant prostate cancer treated with long-term androgen deprivation therapy, which leads to decreased PSMA expression that limits detection of metastatic lesions by PSMA PET/CT [40, 41]. Similar to the role of MY-RADS in MM evaluation, the ex-

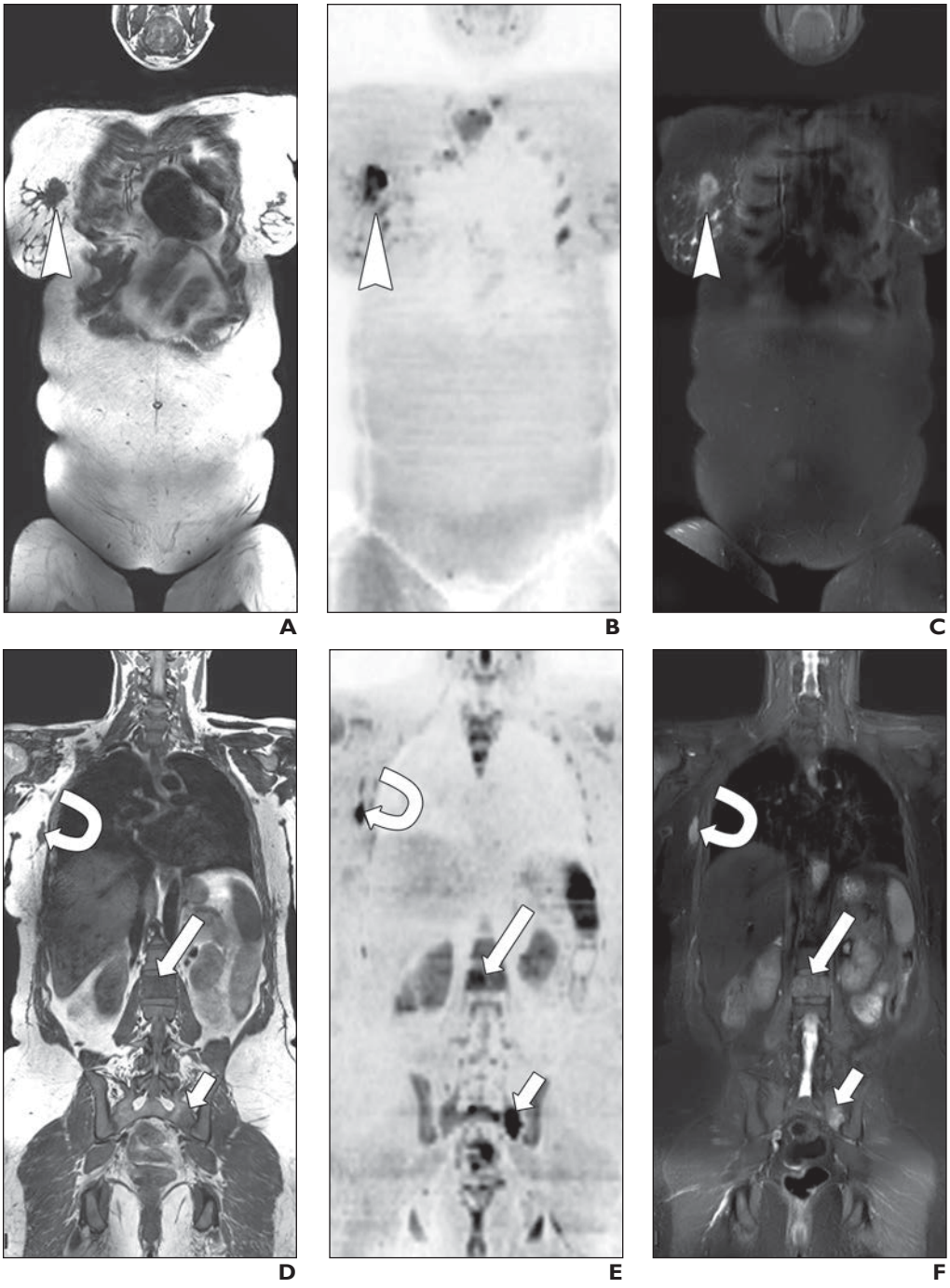


**Fig. 2**—45-year-old patient with newly diagnosed breast cancer who underwent whole-body MRI (WB-MRI).
**A,** Coronal T1-weighted image shows spiculated right breast mass (*arrowhead*).
**B** and **C,** Coronal DWI (b = 1000 s/mm$^2$; inverted gray-scale) (**B**) and coronal STIR image (**C**) show hyperintensity of mass (*arrowheads*).
**D,** Coronal T1-weighted image, obtained posterior to slice position of **A**–**C**, shows right axillary lymphadenopathy (*curved arrow*) and bone metastases within L2 vertebral body (*long straight arrow*) and left sacral wing (*short straight arrow*).
**E** and **F,** Coronal DWI (**E**) and coronal STIR image (**F**) show right axillary lymphadenopathy (*curved arrows*), L2 lesion (*long straight arrows*), and left sacral lesion (*short straight arrows*). Findings indicate promising role of WB-MRI in determining TNM categories for cancer staging through single imaging examination.

pert-designed Metastasis Reporting and Data System standardizes the acquisition and interpretation of WB-MRI for prostate cancer evaluation and allows WB-MRI to serve as a quantifiable biomarker in clinical trials [42]. In addition to visceral malignancies, WB-MRI is also useful in patients with MLS [43, 44]; unlike other liposarcomas, MLS has a propensity to metastasize to bone and soft tissues before metastasizing to the lungs. WB-MRI can detect extrapulmonary lesions that may otherwise be occult on conventional surveillance imaging [45, 46]. Limitations of WB-MRI in the detection of metastases from visceral organ malignancies include suboptimal specificity and, despite advances in free-breathing 3D MRI sequences, continued reliance on chest CT as radiologic surveillance for pulmonary metastases [47].

WB-MRI has emerged as a versatile tool for pediatric oncologic imaging, providing a nonionizing method of evaluation for metastatic disease with high diagnostic performance. The Oncology Task Force of the European Society of Pediatric Radiology recommends WB-MRI as a first- or second-line tool in the management of children with non–FDG-avid lymphoma, neuroblastoma, sarcoma, and Langerhans cell histiocytosis (LCH) [48]. A

**TABLE 2: Qualitative and Quantitative Whole-Body MRI Sequences and Their Roles**

| Category | Sequence Options | Role |
|---|---|---|
| Core sequences | | |
| T1-weighted (fat-sensitive) | Sagittal and/or axial 2D T1-weighted FSE sequence using 4- to 5-mm ST<br>Axial and/or coronal 2D T1-weighted GRE Dixon sequence using 5-mm ST<br>3D FSE T1-weighted GRE Dixon sequence<br>Axial or coronal 2D T1-weighted FSE Dixon sequence using 4- to 5-mm ST, providing in-phase and fat-only images[a] | Detection of focal sites of skeletal disease<br>Characterization of marrow pattern (normal, focal, focal-on-diffuse, diffuse, or micronodular)<br>Qualitative assessment of treatment response |
| T2-weighted (fluid-sensitive) | Sagittal, axial, or coronal 2D T2-weighted FS sequence with 5-mm ST<br>Sagittal, axial, or coronal 2D STIR sequence with 5-mm ST<br>Sagittal or coronal 2D T2-weighted Dixon sequence using 5-mm ST<br>3D FSE single-slab T2-weighted sequence<br>Coronal or axial 2D T2-weighted FSE Dixon sequence using 4- to 5-mm ST, providing water-only images[b] | Detection of soft-tissue, nodal, or visceral disease<br>Qualitative assessment of treatment response |
| DWI with ADC map | Axial 2D DWI using STIR FS sequence with 5-mm ST and two or three b values (50–100 and 800–1000 s/mm$^2$; optional, 400–600 s/mm$^2$)<br>Postprocessed ADC map using two or more b values and monoexponential fit | Low-b-value DWI: detection of skeletal, soft-tissue, nodal, or visceral abnormalities<br>High-b-value DWI: detection of active skeletal disease<br>Characterization of disease using qualitative absence of signal loss from low- to high-b-value DWI or low signal on ADC map as an indicator of restricted diffusion<br>Assessment of treatment response |
| Adjunct sequences | | |
| Postcontrast sequences | Axial, sagittal, or coronal T1-weighted FS<br>Axial, sagittal, or coronal FS VIBE | Increased lesion conspicuity<br>Lesion characterization |
| Dixon sequences for FF quantification | Axial and/or coronal 2D T1-weighted GRE Dixon sequence using 5-mm ST<br>3D T1-weighted GRE Dixon sequence with FF map<br>For either 2D or 3D method, FF map from water-only and fat-only images | Characterization of bone marrow abnormalities (differentiation of diffuse marrow infiltration [lower FF] from hematopoietic or normal bone marrow [higher FF])<br>Quantification of disease severity or skeletal muscle damage in congenital myopathy<br>Assessment of treatment response |

Note—FSE = fast spin-echo, ST = slice thickness, GRE = gradient-recalled echo, FS = fat saturation, FF = fat fraction.
[a]Choice of optimal acquisition plane depends on indication (i.e., oncology, inflammation, or neuromuscular disorder).
[b]A single T2-weighted FSE Dixon sequence provides fat-sensitive (fat-only), fluid-sensitive (water-only), and anatomic (in-phase) images. In addition, quantitative data may be derived through measurement of signal drop or through reconstruction of FF maps.

meta-analysis of 118 pediatric patients with various malignancies revealed a sensitivity of 96% and specificity of 90% for the detection of metastatic disease. Another study showed high diagnostic accuracy of WB-MRI in the detection of skip metastases in patients with peripheral osteosarcoma and Ewing sarcoma [49]. In a further study of patients with Ewing sarcoma, WB-MRI had higher sensitivity than bone scintigraphy for the detection of skeletal metastases, with the exception of calvarial metastases [50]. In patients with LCH, the number of lesions impacts management. In one study, WB-MRI had higher sensitivity than bone scintigraphy and skeletal survey in lesion detection in patients with LCH, although the modalities had no statistically significant difference in initial disease stratification [43]. A limitation of WB-MRI in children is the potential need to sedate the patient during the examination, given the examination's long acquisition times, to prevent motion artifacts. Interpretation may also be difficult related to the physiologic heterogeneity of bone marrow in children.

Finally, WB-MRI can impact management of a pregnant patient with malignancy, including staging of cancer and searching for a primary disease site when cancer is detected incidentally (e.g., by noninvasive prenatal testing [NIPT]). Unenhanced MRI during pregnancy is generally considered safe for the fetus, especially in the second or third trimester [44]. The presence of maternal malignancy during pregnancy can result in false-positive NIPT due to multiple chromosomal aneuploidies [51]. In pregnant patients, unenhanced WB-MRI using DWI can identify a previously unknown site of primary malignancy, detect nodal or distal metastases, and serve as surveillance with higher diagnostic performance than conventional imaging (composed of breast ultrasound and/or mammography, spine MRI, abdominal ultrasound, and potentially chest CT) [52].

WB-MRI, particularly in conjunction with DWI, is increasingly accepted as a method of detecting metastatic disease, as it can simultaneously evaluate visceral, nodal, and skeletal metastases. Unlike bone scintigraphy or PET, WB-MRI does not rely on the affinity of a particular radiotracer to underlying histologic properties of the tumor. The combination of anatomic fat- and fluid-sensitive sequences with physiologic techniques (e.g., DWI) allows WB-MRI to be applied widely for the assessment of soft-tissue and skeletal sites of disease regardless of the site of primary malignancy [2]. Table 2 summarizes various WB-MRI sequences and their role in the evaluation of disease extent and treatment deter-

mination. Importantly, small pulmonary metastases can be challenging to detect via WB-MRI.

### *Nononcologic Applications*

Nononcologic indications for WB-MRI are limited and predominantly applied in clinical trials rather than in clinical care settings. Nononcologic indications include multifocal aseptic musculoskeletal disorders such as chronic recurrent multifocal osteomyelitis (CRMO) or CNO, SAPHO, congenital or inflammatory myopathy, inflammatory arthritis, and FUO [5, 53–55].

In patients with CNO, WB-MRI can reveal asymptomatic disease sites that would otherwise be clinically occult [56–58]. In a prospective investigation, WB-MRI detected a greater number of active lesions than did clinical assessment in approximately half of patients [56]. An additional study showed the use of WB-MRI as a biomarker for disease activity and treatment response in CRMO [55]. In retrospective studies, WB-MRI showed treatment response and disease progression after the administration of bisphosphonates in patients with CNO who were unresponsive to NSAIDs [57, 58]. Similarly, WB-MRI can detect disease activity and assess treatment response in adult patients with SAPHO and in most European centers has replaced bone scintigraphy for the evaluation of patients with CRMO and SAPHO [59].

WB-MRI has also been explored for the assessment of congenital myopathy and inflammatory myopathy (Fig. 3). In children with dermatomyositis, WB-MRI detects additional sites of muscle involvement in comparison with clinical assessment alone and may be used for treatment response assessment [60–62]. In addition, myofascial involvement, as detected by WB-MRI, can serve as a marker for rapidly progressive interstitial lung disease in patients with dermatomyositis [63]. However, it is unknown whether WB-MRI is superior to localized MRI of the pelvis and thighs or localized MRI of the shoulder girdle, which are commonly performed for diagnosis and treatment response assessment in patients with inflammatory myopathy. Although WB-MRI is not routinely performed clinically for evaluation of inflammatory myopathy in the United States, WB-MRI including axial T2-weighted Dixon sequences with coverage extending from the neck to ankles is routinely performed for the evaluation of inflammatory myopathy in Europe [5, 64, 65]. The use of a single axial fast spin-echo (FSE) T2-weighted sequence allows total-body assessment of muscular fatty infiltration and edema in 20–25 minutes [66].

WB-MRI can provide insight into patterns of muscle involvement in patients with congenital myopathy [67, 68]. In addition, in patients with Duchenne muscular dystrophy and spinal muscular atrophy, quantitative measurements of intramuscular fat mass derived from WB-MRI have been shown to be more accurate than fat mass estimates calculated based on anthropometric measurements [69, 70]. With emerging deep learning algorithms, WB-MRI can be used to quantify muscle bulk in dystrophic and nondystrophic skeletal muscles in patients with congenital myopathy such as limb girdle muscular dystrophy resulting from variants in the *FKRP* gene; WB-MRI can also serve as a biomarker for disease severity and therapeutic response in clinical trial [71].

In patients with axial spondyloarthritis, WB-MRI enables detection of clinically occult inflammatory lesions and provides simultaneous evaluation of the axial and appendicular skeletons [72, 73]. WB-MRI has been explored for assessment of treatment response and remission after golimumab treatment, in one study showing a decrease in inflammation in the axial and appendicu-

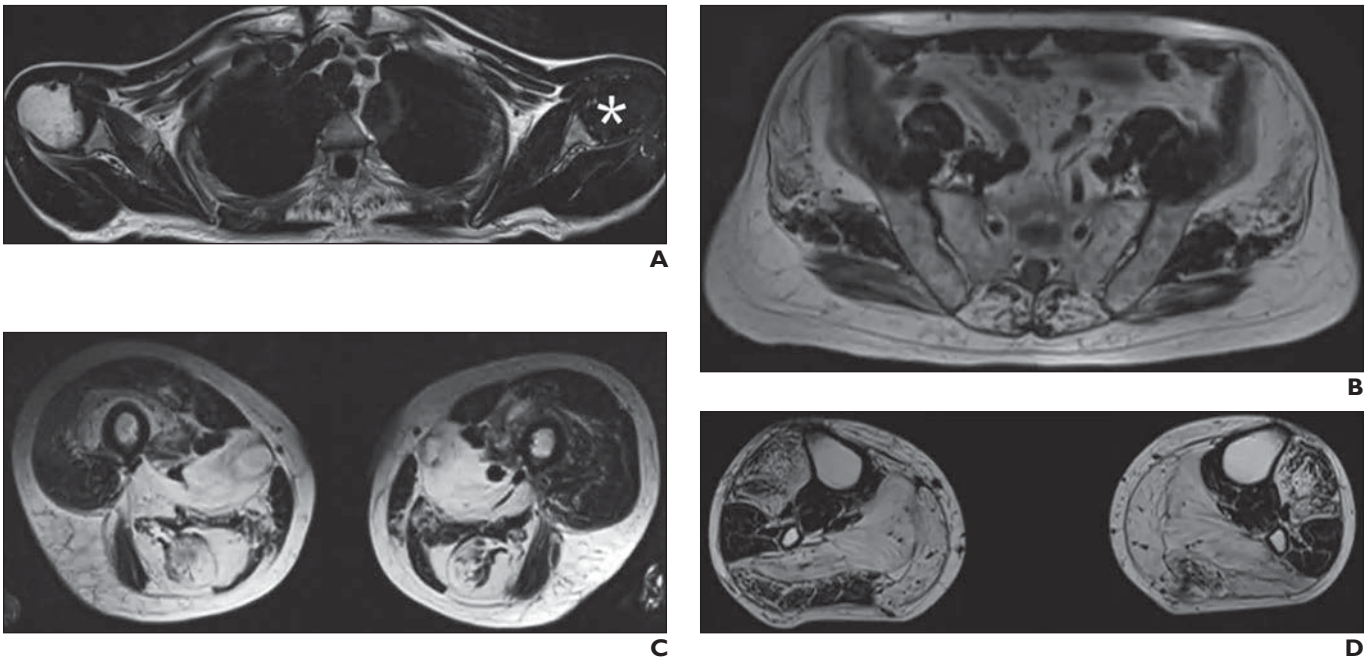


**Fig. 3**—70-year-old patient with limb girdle muscular dystrophy who underwent whole-body MRI examination that included axial fast spin-echo T2-weighted Dixon sequences.
**A–D,** Fat-only images of shoulder girdle (**A**), pelvic girdle (**B**), proximal lower extremity (**C**), and distal lower extremity (**D**) show fatty infiltration of muscles of pelvic girdle (**B**) and lower limbs (**C** and **D**), without significant atrophy. Fat-water swapping artifact (*asterisk*, **A**) is noted.

**(Fig. 3 continues on next page)**

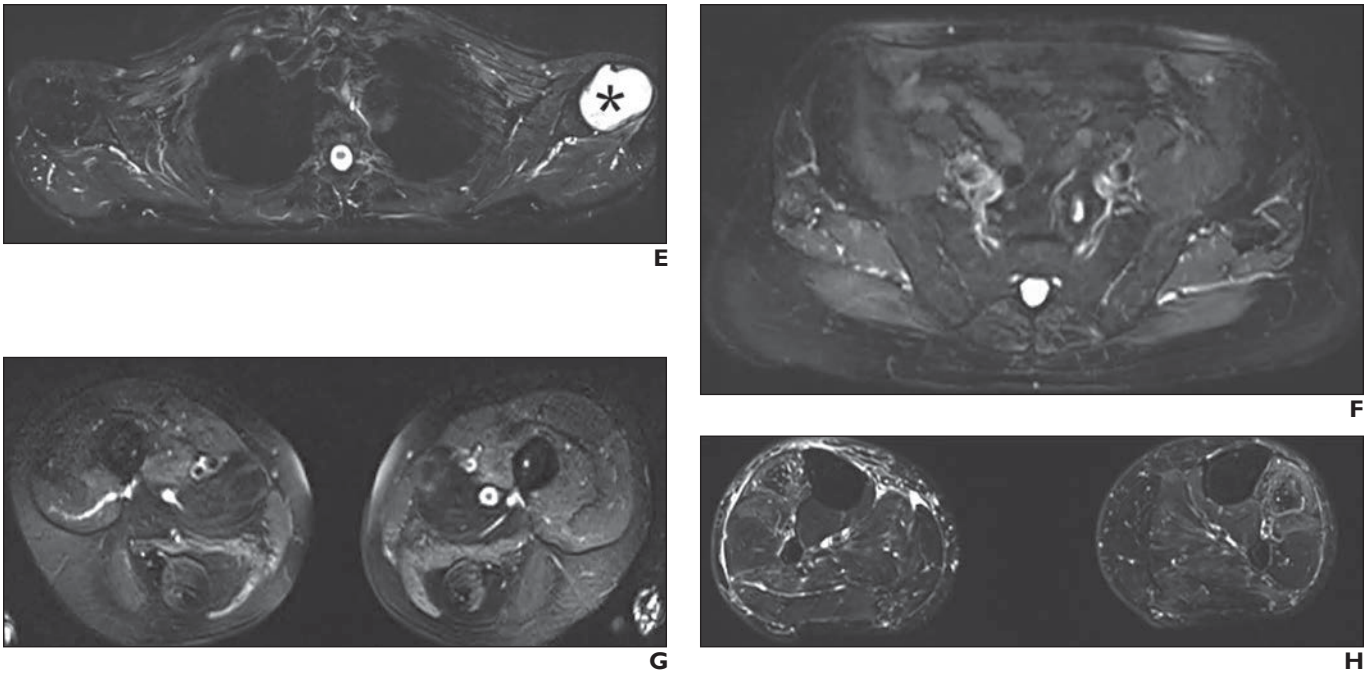


**Fig. 3 (continued)—**70-year-old patient with limb girdle muscular dystrophy who underwent whole-body MRI examination that included axial fast spin-echo T2-weighted Dixon sequences.
**E–H,** Water-only images of shoulder girdle (**E**), pelvic girdle (**F**), proximal lower extremity (**G**), and distal lower extremity (**H**). Fat-only and water-only images allow assessment of presence and distribution of fatty infiltration and muscle edema, respectively. Areas of muscle edema are present in anterior compartments of distal lower extremities (**H**), which were targeted for biopsy. Fat-water swapping artifact (*asterisk*, **E**) is noted.

lar skeletons as well as in the entheses [72, 73]. In a study of patients with early axial spondyloarthritis, clinical assessment was superior to WB-MRI using routine unenhanced T1-weighted and STIR sequences [74]. However, in another study of patients with active axial spondyloarthritis, WB-MRI including DWI detected more sites of active inflammation than WB-MRI using STIR sequences alone [75]. In contrast with the observations in early axial spondyloarthritis, in a study of patients with psoriatic arthritis, WB-MRI performed before and after IV contrast material administration was superior to clinical examination for the detection of inflammatory lesions such as enthesitis (with the exception of synovitis or dactylitis in the hands and feet) [76]. In a further study, clinically occult inflammatory lesions detected by WB-MRI altered the therapeutic plan in 73.3% of patients with psoriatic arthritis [76]. The inflammation index derived from WB-MRI is being investigated as a primary endpoint in clinical trials assessing treatment response in patients with axial spondyloarthritis, and the Outcome Measures in Rheumatology (OMERACT) working group is exploring the standardization of WB-MRI sequences and imaging planes, as well as the development of a preliminary scoring system for inflammation on WB-MRI [77, 78]. Despite these advancements, WB-MRI is not routinely performed clinically for the assessment of seronegative spondyloarthropathy.

In a single-center study of 92 children with fever without a focus, WB-MRI was informative in 67.4% of children, particularly in immunosuppressed children [79]. In an additional study, unenhanced WB-MRI using conventional sequences and DWI identified the correct diagnosis in 70% of patients with FUO and was the only modality to detect the inflammatory focus in approximately half of patients [80]. Furthermore, in a single-center study of patients with multifocal osteonecrosis, whole-body bone scintigraphy detected 82.6% of symptomatic lesions and 21.7% of asymptomatic lesions detected by WB-MRI [81]. The utility of detecting asymptomatic lesions by WB-MRI is unknown.

Although nononcologic applications for WB-MRI are increasing and the modality's use in myositis and CRMO is gaining acceptance, WB-MRI is not a routine diagnostic tool for the clinical care of musculoskeletal inflammatory disorders as of November 2022 [5].

## Imaging Protocol

Variations in imaging planes, sequences, and sequence parameters have resulted in heterogeneous WB-MRI protocols [5]. Table 2 shows current sequences in WB-MRI protocols and justifications for their use. For institutions performing WB-MRI for a spectrum of indications (Table 1), we recommend implementing a core protocol aimed at answering clinical questions common to most or all indications and adding sequences on the basis of specific needs of select patient populations. Because most WB-MRI indications require bone marrow assessment, the core protocol should include T1-weighted sequences, T2-weighted sequences, and DWI sequences extending from the vertex to knees [82]. Recent surveys of WB-MRI implementation have shown these are the most commonly used sequences, reflecting the dominant use of WB-MRI for assessment of skeletal disease [5, 83]. The combination of T1-weighted and STIR sequences can alternatively be replaced by a single T2-weighted Dixon sequence [84]. The core protocol and anatomic coverage can be modified for disease-specific indications. For example, the coverage can extend from the vertex to the toes in patients with LFS to maximize detection of soft-tissue and bone sarcomas as well as in patients

with myopathy to visualize the calf musculature. WB-MRI can be performed on either 1.5-T or 3-T systems using surface coils specific to the imaged anatomic sites to maximize SNR [22, 23]. Given the impact of a range of scanner-related factors, serial examinations in an individual patient should be performed on the same system using the same technique. A simplified protocol designed to detect bone marrow disease in patients with MM can be performed in 30 minutes. The incorporation of additional sequences to evaluate treatment response or the modification of anatomic coverage in patients with other conditions such as LFS can increase table time to 60 minutes, if not longer [23].

Fat-only images derived from gradient-recalled echo T1-weighted Dixon sequences offer an alternative to FSE T1-weighted sequences for marrow evaluation given their increased specificity for marrow-replacing processes as well as the method's substantial time savings [20, 21]. FSE T2-weighted Dixon sequences, although not as fast as T1-weighted Dixon sequences, can provide both fat- (i.e., marrow-) and fluid-sensitive images in a single acquisition, with robust fat suppression [85]. Dixon-based techniques can also quantify the degree of marrow replacement through FF calculation, improve specificity for neoplasm detection, and quantify treatment response [27–29].

Contrast agents are not routinely administered in WB-MRI examinations. Nonetheless, postcontrast images can have increased lesion conspicuity in patients with cancer predisposition syndromes or with known malignancies, can highlight areas of active disease in inflammatory conditions, and can improve detection and characterization of lung, liver, brain, and bone lesions [86]. Contrast material should be routinely administered when performing additional dedicated brain imaging in the same session as the WB-MRI [87].

## Controversies

WB-MRI has been incorporated into professional society guidelines and expert recommendations. Nonetheless, obstacles are associated with its incorporation into routine clinical workflow, including limited availability or access to the technology, incidental and/or false-positive findings, uncertain cost-effectiveness, and potential billing difficulties.

WB-MRI acquisition and interpretation can be challenging. Thus, in the United States, WB-MRI is not routinely available at most radiology practices but rather is typically performed at tertiary referral centers. This limited access may hinder adherence to staging and surveillance guidelines that include WB-MRI. Instead of WB-MRI, MRI of the axial skeleton (i.e., of the entire spine and pelvis) may be performed as an alternative, but this approach can miss extraaxial sites of disease that would impact diagnostic reasoning and alter the treatment paradigm, especially in patients with MM. Whole-body FDG PET/CT is an additional alternative first-line method but is limited in certain patient populations, such as those with indolent lymphoma or MLS. High-quality prospective randomized multicenter data supporting the added value of WB-MRI would increase recognition and acceptance of the technology.

Patient access to WB-MRI may be impacted not only by scanner availability but also by examination duration. The increasing adoption of gradient-recalled echo T1-weighted Dixon sequences, FSE T2-weighted Dixon sequences, isotropic volumetric 3D sequences, and simultaneous multislice free-breathing DWI sequences will help decrease WB-MRI acquisition times [88, 89]. Patient claustrophobia is an additional challenge in implementing WB-MRI [90]. Yet, in one study, despite lengthy acquisition times, most patients with lung or colorectal cancer undergoing WB-MRI reported a willingness to undergo an additional WB-MRI examination if necessary [90].

WB-MRI interpretation requires expertise. Professional organizations have developed structured reporting systems for WB-MRI for MM, prostate cancer, and nononcologic indications such as axial spondyloarthritis. Tewattanarat et al. [91] recommended consensus double-reading of WB-MRI examinations to help classify indeterminate examinations and potentially improve diagnostic accuracy. In one study, centralized interpretation of WB-MRI with DWI achieved higher diagnostic accuracy for the detection of skeletal metastases in comparison with onsite interpretation (87% vs 80%) [92]. Yet, although onsite interpretation achieved higher sensitivity than central interpretation (57% vs 43%), specificity was lower (83% vs 94%) [93]. Based on Society of Skeletal Radiology survey results, WB-MRI in clinical practice is typically interpreted by musculoskeletal radiologists, with consultation as needed with neuroradiologists or abdominal radiologists for indeterminate findings [86].

Incidental findings are common on WB-MRI and impact resource utilization and cost. Clinically significant incidental findings (Fig. 4) have been reported on WB-MRI with a frequency ranging from 8.1% to 14.3% [92, 94, 95]. In a large retrospective study of asymptomatic adults, WB-MRI yielded several important findings warranting therapeutic interventions, including invasive cancers and intracranial aneurysms [96]. In addition to incidental findings, false-positive findings for bone lesions also affect overall costs due to additional diagnostic tests and expert consultation. The use of quantitative methods, such as ADC values or FF from chemical-shift imaging, may help decrease false-positive detection of marrow and soft-tissue lesions in WB-MRI [28, 97].

An evaluation of the cost-effectiveness of WB-MRI in patients with lung and colon cancer from the National Health System in the United Kingdom indicated that WB-MRI is more cost-effective than conventional imaging for staging metastatic disease [90]. A similar cost-effectiveness analysis in patients with LFS indicated that a cancer surveillance program that includes WB-MRI is cost-effective for the early detection of asymptomatic cancers [98]. On the other hand, a study in the French health care system found WB-MRI to be less cost-effective than whole-body $^{18}$F-labeled sodium fluoride PET/CT for the evaluation of patients with prostate cancer with first biochemical recurrence and no ongoing androgen-deprivation treatment [93]. Although PET/CT is more available and in some clinical scenarios is more cost-effective than WB-MRI, PET/CT may not be the preferred test in young patients with cancer predispositions and heightened radiation sensitivity, may not be suitable for certain tumor histologies, and may not be appropriate in pregnant patients.

Additional controversies include the relative timing of when to perform localized MRI versus WB-MRI; the need to perform potential repeated administrations of IV contrast material in certain disease conditions, whether for localized MRI or WB-MRI; and the uncertain diagnostic performance of WB-MRI relative to PET/MRI.

Reimbursement for WB-MRI varies across nations and can present a challenge for implementing WB-MRI in clinical prac-

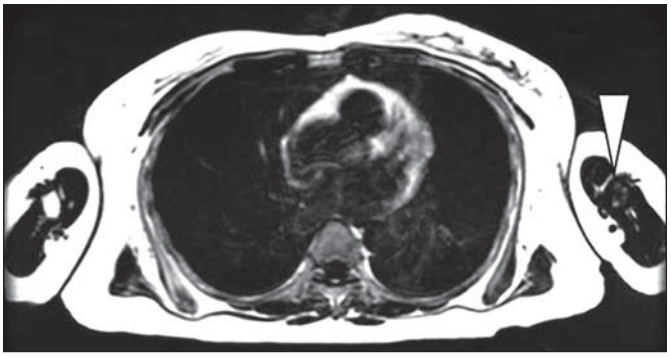

A

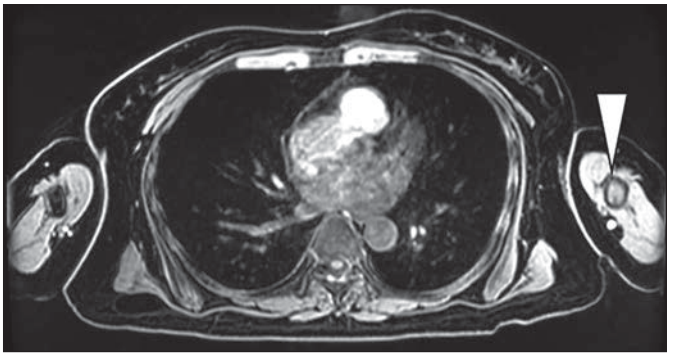

B

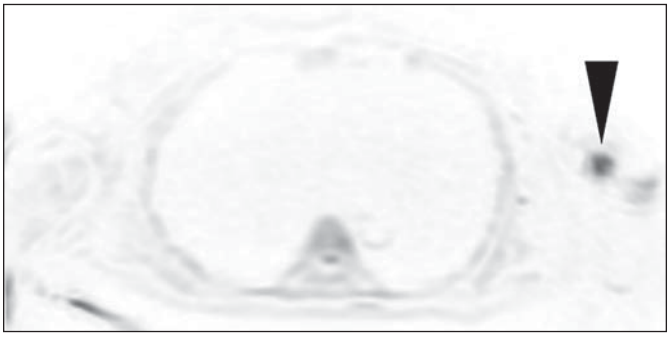

C

**Fig. 4**—62-year-old patient who underwent whole-body MRI for restaging of multiple myeloma. Patient also had history of gallbladder adenocarcinoma.
**A,** Axial T1-weighted Dixon fat-only image shows marrow-replacing lesion in left humerus (*arrowhead*).
**B,** Corresponding axial water-only image also shows lesion (*arrowhead*).
**C,** DWI (b = 800 s/mm$^2$; inverted gray-scale) shows corresponding hyperintensity (*arrowhead*). Note difference in appearance of lesion compared with normal marrow in contralateral right humerus. Subsequent biopsy showed lesion to represent gallbladder adenocarcinoma metastasis.

tice. In the United States, no dedicated CPT code currently exists for WB-MRI. CPT code 77084 describes MRI of the bone marrow blood supply (i.e., MRI for bone marrow survey) and can be used to bill WB-MRI. Based on national Medicare rates, CPT code 77084 is reimbursed approximately $976.10 (technical component of $830.94 and professional component of $145.16), comparable to the reimbursement of approximately $830.45 for an unenhanced cervical spine MRI (technical component of $664.36 and professional component of $166.09) [99]. A code related to bone marrow evaluation may not be optimal when performing WB-MRI to evaluate extra skeletal disease sites such as in the setting of LFS, NF1, and MLS. Current actual billing practices for WB-MRI in the United States are variable, with many academic institutions and private practices billing WB-MRI using the combination of codes for chest MRI, MRI of the abdomen, and MRI of the pelvis or using unlisted MRI codes [100].

## Consensus Opinions

- WB-MRI is an established screening tool for the early detection of malignancy in patients with genetic cancer predisposition syndromes; the strongest available evidence supports the role of WB-MRI in LFS.
- WB-MRI protocols should include T1-weighted sequences, T2-weighted and STIR sequences, and DWI for optimal lesion detection and characterization. Dixon sequences may also be performed for fat quantification. ADC values and FFs may help quantify disease burden and assess treatment response.
- Dixon sequences and other acceleration methods can be used to reduce WB-MRI acquisition times.
- Given the impact of scanner-related factors, serial WB-MRI examinations should be performed on the same magnet using the same technique.
- International guidelines for management of MM incorporate WB-MRI. When available, WB-MRI should be considered the first-line modality in the initial workup, staging, response evaluation, and surveillance of patients with MM.
- WB-MRI can be used for the detection of metastatic disease in patients with known visceral malignancies (e.g., prostate cancer), soft-tissue or bone neoplasms (e.g., MLS, Ewing sarcoma, osteosarcoma, LCH), and non–FDG-avid lymphomas.
- In pregnant patients with malignancy, WB-MRI should be considered as a first-line modality for the detection of an unknown primary site of cancer and for staging of known and incidentally detected malignancies.
- WB-MRI should be considered a first- or second-line modality in children with non–FDG-avid lymphoma, neuroblastoma, soft-tissue or bone sarcoma, and LCH.
- WB-MRI has been explored for nononcologic indications such as aseptic musculoskeletal disorders, inflammatory or congenital myopathy, inflammatory arthritis, and FUO.
- As of November 2022, no dedicated CPT code exists for describing WB-MRI examinations, leading to variable approaches for billing such studies and potential implementation barriers. More clearly defined pathways for billing WB-MRI examinations would facilitate appropriate utilization.

**Provenance and review:** Solicited; externally peer reviewed.

**Peer reviewers:** Jeffrey A. Belair, Thomas Jefferson University; Hyun Su Kim, Samsung Medical Center; additional individuals who chose not to disclose their identities.

## References

1. Lecouvet FE, Michoux N, Nzeusseu Toukap A, et al. The increasing spectrum of indications of whole-body MRI beyond oncology: imaging answers to clinical needs. *Semin Musculoskelet Radiol* 2015; 19:348–362
2. Lecouvet FE. Whole-body MR imaging: musculoskeletal applications. *Radiology* 2016; 279:345–365
3. Barakat E, Kirchgesner T, Triqueneaux P, Galant C, Stoenoiu M, Lecouvet FE. Whole-body magnetic resonance imaging in rheumatic and systemic diseases: from emerging to validated indications. *Magn Reson Imaging Clin N Am* 2018; 26:581–597
4. Jurik AG, Klicman RF, Simoni P, Robinson P, Teh J. SAPHO and CRMO: the value of imaging. *Semin Musculoskelet Radiol* 2018; 22:207–224
5. Giraudo C, Lecouvet FE, Cotten A, et al. Whole-body magnetic resonance imaging in inflammatory diseases: where are we now? Results of an international survey by the European Society of Musculoskeletal Radiology. *Eur J Radiol* 2021; 136:109533
6. Petralia G, Koh DM, Attariwala R, et al. Oncologically relevant findings reporting and data system (ONCO-RADS): guidelines for the acquisition, interpretation, and reporting of whole-body MRI for cancer screening. *Radiology* 2021; 299:494–507
7. Petralia G, Padhani AR, Pricolo P, et al.; Italian Working Group on Magnetic Resonance. Whole-body magnetic resonance imaging (WB-MRI) in oncology: recommendations and key uses. *Radiol Med (Torino)* 2019; 124:218–233
8. Lustbader ED, Williams WR, Bondy ML, Strom S, Strong LC. Segregation analysis of cancer in families of childhood soft-tissue-sarcoma patients. *Am J Hum Genet* 1992; 51:344–356
9. Kleinerman RA. Radiation-sensitive genetically susceptible pediatric sub-populations. *Pediatric Radiol* 2009; 39(suppl 1):S27–S31
10. Ballinger ML, Best A, Mai PL, et al. Baseline surveillance in Li-Fraumeni syndrome using whole-body magnetic resonance imaging: a meta-analysis. *JAMA Oncol* 2017; 3:1634–1639
11. Villani A, Shore A, Wasserman JD, et al. Biochemical and imaging surveillance in germline *TP53* mutation carriers with Li-Fraumeni syndrome: 11 year follow-up of a prospective observational study. *Lancet Oncol* 2016; 17:1295–1305
12. Anupindi SA, Bedoya MA, Lindell RB, et al. Diagnostic performance of whole-body MRI as a tool for cancer screening in children with genetic cancer-predisposing conditions. *AJR* 2015; 205:400–408
13. Bojadzieva J, Amini B, Day SF, et al. Whole body magnetic resonance imaging (WB-MRI) and brain MRI baseline surveillance in *TP53* germline mutation carriers: experience from the Li-Fraumeni Syndrome Education and Early Detection (LEAD) clinic. *Fam Cancer* 2018; 17:287–294
14. Consul N, Amini B, Ibarra-Rovira JJ, et al. Li-Fraumeni syndrome and whole-body MRI screening: screening guidelines, imaging features, and impact on patient management. *AJR* 2021; 216:252–263
15. Ahlawat S, Fayad LM, Khan MS, et al.; Whole Body MRI Committee for the REiNS International Collaboration; REiNS International Collaboration Members 2016. Current whole-body MRI applications in the neurofibromatoses: NF1, NF2, and schwannomatosis. *Neurology* 2016; 87(7 suppl 1):S31–S39
16. Mautner VF, Asuagbor FA, Dombi E, et al. Assessment of benign tumor burden by whole-body MRI in patients with neurofibromatosis 1. *Neuro Oncol* 2008; 10:593–598
17. Rednam SP, Erez A, Druker H, et al. Von Hippel-Lindau and hereditary pheochromocytoma/paraganglioma syndromes: clinical features, genetics, and surveillance recommendations in childhood. *Clin Cancer Res* 2017; 23:e68–e75
18. Jasperson KW, Kohlmann W, Gammon A, et al. Role of rapid sequence whole-body MRI screening in SDH-associated hereditary paraganglioma families. *Fam Cancer* 2014; 13:257–265
19. Jurik AG, Jørgensen PH, Mortensen MM. Whole-body MRI in assessing malignant transformation in multiple hereditary exostoses and enchondromatosis: audit results and literature review. *Skeletal Radiol* 2001; 49:115–124
20. Hillengass J, Usmani S, Rajkumar SV, et al. International Myeloma Working Group consensus recommendations on imaging in monoclonal plasma cell disorders. *Lancet Oncol* 2019; 20:e302–e312
21. Messiou C, Hillengass J, Delorme S, et al. Guidelines for acquisition, interpretation, and reporting of whole-body MRI in myeloma: Myeloma Response Assessment and Diagnosis System (MY-RADS). *Radiology* 2019; 291:5–13
22. Messiou C, Porta N, Sharma B, et al. Prospective evaluation of whole-body MRI versus FDG PET/CT for lesion detection in participants with myeloma. *Radiol Imaging Cancer* 2021; 3:e210048
23. Wu F, Bernard S, Fayad LM, et al. Updates and ongoing challenges in imaging of multiple myeloma: *AJR* expert panel narrative review. *AJR* 2021; 217:775–785
24. Wang D, Huo Y, Chen S, et al. Whole-body MRI versus $^{18}$F-FDG PET/CT for pretherapeutic assessment and staging of lymphoma: a meta-analysis. *Onco Targets Ther* 2018; 11:3597–3608
25. Lin G, Zong X, Li Y, et al. Whole-body MRI is an effective imaging modality for hematological malignancy treatment response assessment: a systematic review and meta-analysis. *Front Oncol* 2022; 12:827777
26. Lecouvet FE, Vekemans MC, Van Den Berghe T, et al. Imaging of treatment response and minimal residual disease in multiple myeloma: state of the art WB-MRI and PET/CT. *Skeletal Radiol* 2022; 51:59–80
27. Omoumi P. The Dixon method in musculoskeletal MRI: from fat-sensitive to fat-specific imaging. *Skeletal Radiol* 2022; 51:1365–1369
28. Sun M, Cheng J, Ren C, et al. Differentiation of diffuse infiltration pattern in multiple myeloma from hyperplastic hematopoietic bone marrow: qualitative and quantitative analysis using whole-body MRI. *J Magn Reson Imaging* 2022; 55:1213–1225
29. Dong H, Huang W, Ji X, et al. Prediction of early treatment response in multiple myeloma using MY-RADS total burden score, ADC, and fat fraction from whole-body MRI: impact of anemia on predictive performance. *AJR* 2022; 218:310–319
30. Takasu M, Tanitame K, Baba Y, et al. Does chemical shift imaging offer a biomarker for the diagnosis and assessment of disease severity in multiple myeloma? A cross-sectional study. *Medicine (Baltimore)* 2021; 100:e24358
31. Machado Medeiros T, Altmayer S, Watte G, et al. $^{18}$F-FDG PET/CT and whole-body MRI diagnostic performance in M staging for non-small cell lung cancer: a systematic review and meta-analysis. *Eur Radiol* 2020; 30:3641–3649
32. Pasoglou V, Van Nieuwenhove S, Van Damme J, et al. Whole body MRI in the detection of lymph node metastases in patients with testicular germ cell cancer. *Life (Basel)* 2022; 12:212
33. Lecouvet FE, El Mouedden J, Collette L, et al. Can whole-body magnetic resonance imaging with diffusion-weighted imaging replace Tc 99m bone scanning and computed tomography for single-step detection of metastases in patients with high-risk prostate cancer? *Eur Urol* 2012; 62:68–75
34. Taylor SA, Mallett S, Beare S, et al.; Streamline Investigators. Diagnostic accuracy of whole-body MRI versus standard imaging pathways for metastatic disease in newly diagnosed colorectal cancer: the prospective Streamline C trial. *Lancet Gastroenterol Hepatol* 2019; 4:529–537

35. Kosmin M, Padhani AR, Sokhi H, Thijssen T, Makris A. Patterns of disease progression in patients with local and metastatic breast cancer as evaluated by whole-body magnetic resonance imaging. *Breast* 2018; 40:82–84
36. Noij DP, Boerhout EJ, Pieters-van den Bos IC, et al. Whole-body-MR imaging including DWIBS in the work-up of patients with head and neck squamous cell carcinoma: a feasibility study. *Eur J Radiol* 2014; 83:1144–1151
37. De Vuysere S, Vandecaveye V, De Bruecker Y, et al. Accuracy of whole-body diffusion-weighted MRI (WB-DWI/MRI) in diagnosis, staging and follow-up of gastric cancer, in comparison to CT: a pilot study. *BMC Med Imaging* 2021; 21:18
38. Petralia G, Padhani A, Summers P, et al. Whole-body diffusion-weighted imaging: is it all we need for detecting metastases in melanoma patients? *Eur Radiol* 2013; 23:3466–3476
39. Bhaludin BN, Tunariu N, Koh DM, et al. A review on the added value of whole-body MRI in metastatic lobular breast cancer. *Eur Radiol* 2022; 32:6514–6525
40. Liu T, Wu LY, Fulton MD, Johnson JM, Berkman CE. Prolonged androgen deprivation leads to downregulation of androgen receptor and prostate-specific membrane antigen in prostate cancer cells. *Int J Oncol* 2012; 41:2087–2092
41. Afshar-Oromieh A, Debus N, Uhrig M, et al. Impact of long-term androgen deprivation therapy on PSMA ligand PET/CT in patients with castration-sensitive prostate cancer. *Eur J Nucl Med Mol Imaging* 2018; 45:2045–2054
42. Padhani AR, Lecouvet FE, Tunariu N, et al. Metastasis Reporting and Data System for prostate cancer: practical guidelines for acquisition, interpretation, and reporting of whole-body magnetic resonance imaging-based evaluations of multiorgan involvement in advanced prostate cancer. *Eur Urol* 2017; 71:81–92
43. Kim JR, Yoon HM, Jung AY, Cho YA, Seo JJ, Lee JS. Comparison of whole-body MRI, bone scan, and radiographic skeletal survey for lesion detection and risk stratification of Langerhans cell histiocytosis. *Sci Rep* 2019; 9:317
44. Bulas D, Egloff A. Benefits and risks of MRI in pregnancy. *Semin Perinatol* 2013; 37:301–304
45. Visgauss JD, Wilson DA, Perrin DL, et al. Staging and surveillance of myxoid liposarcoma: follow-up assessment and the metastatic pattern of 169 patients suggests inadequacy of current practice standards. *Ann Surg Oncol* 2021; 28:7903–7911
46. Gorelik N, Reddy SMV, Turcotte RE, et al. Early detection of metastases using whole-body MRI for initial staging and routine follow-up of myxoid liposarcoma. *Skeletal Radiol* 2018; 47:369–379
47. Bruckmann NM, Kirchner J, Morawitz J, et al. Free-breathing 3D Stack of Stars GRE (StarVIBE) sequence for detecting pulmonary nodules in $^{18}$F-FDG PET/MRI. *EJNMMI Phys* 2022; 9:11
48. Schäfer JF, Granata C, von Kalle T, et al.; Oncology Task Force of the ESPR. Whole-body magnetic resonance imaging in pediatric oncology: recommendations by the Oncology Task Force of the ESPR. *Pediatr Radiol* 2020; 50:1162–1174
49. Barnett JR, Gikas P, Gerrand C, Briggs TW, Saifuddin A. The sensitivity, specificity, and diagnostic accuracy of whole-bone MRI for identifying skip metastases in appendicular osteosarcoma and Ewing sarcoma. *Skeletal Radiol* 2020; 49:913–919
50. Kalus S, Saifuddin A. Whole-body MRI vs bone scintigraphy in the staging of Ewing sarcoma of bone: a 12-year single-institution review. *Eur Radiol* 2019; 29:5700–5708
51. Amant F, Verheecke M, Wlodarska I, et al. Presymptomatic identification of cancers in pregnant women during noninvasive prenatal testing. *JAMA Oncol* 2015; 1:814–819
52. Han SN, Amant F, Michielsen K, et al. Feasibility of whole-body diffusion-weighted MRI for detection of primary tumour, nodal and distant metastases in women with cancer during pregnancy: a pilot study. *Eur Radiol* 2018; 28:1862–1874
53. Voit AM, Arnoldi AP, Douis H, et al. Whole-body magnetic resonance imaging in chronic recurrent multifocal osteomyelitis: clinical long-term assessment may underestimate activity. *J Rheumatol* 2015; 42:1455–1462
54. Andronikou S, Kraft JK, Offiah AC, et al. Whole-body MRI in the diagnosis of paediatric CNO/CRMO. *Rheumatology (Oxford)* 2020; 59:2671–2680
55. Kieninger A, Schäfer JF, Tsiflikas I, et al. Early diagnosis and response assessment in chronic recurrent multifocal osteomyelitis: changes in lesion volume and signal intensity assessed by whole-body MRI. *Br J Radiol* 2022; 95:20211091
56. Arnoldi AP, Schlett CL, Douis H, et al. Whole-body MRI in patients with non-bacterial osteitis: radiological findings and correlation with clinical data. *Eur Radiol* 2017; 27:2391–2399
57. Roderick M, Shah R, Finn A, Ramanan AV. Efficacy of pamidronate therapy in children with chronic non-bacterial osteitis: disease activity assessment by whole body magnetic resonance imaging. *Rheumatology (Oxford)* 2014; 53:1973–1976
58. Bhat CS, Roderick M, Sen ES, Finn A, Ramanan AV. Efficacy of pamidronate in children with chronic non-bacterial osteitis using whole body MRI as a marker of disease activity. *Pediatr Rheumatol Online J* 2019; 17:35
59. Wang L, Sun B, Li C. Clinical and radiological remission of osteoarticular and cutaneous lesions in SAPHO patients treated with secukinumab: a case series. *J Rheumatol* 2021; 48:953–955
60. Malattia C, Damasio MB, Madeo A, et al. Whole-body MRI in the assessment of disease activity in juvenile dermatomyositis. *Ann Rheum Dis* 2014; 73:1083–1090
61. Matsuda N, Kobayashi S, Hasegawa O, et al. Subclinical involvement of the trunk muscles in idiopathic inflammatory myopathies. *Acta Radiol Open* 2022 Feb 28 [published online]
62. Elessawy SS, Abdelsalam EM, Abdel Razek E, Tharwat S. Whole-body MRI for full assessment and characterization of diffuse inflammatory myopathy. *Acta Radiol Open* 2016 Sep 21 [published online]
63. Karino K, Kono M, Kono M, et al. Myofascia-dominant involvement on whole-body MRI as a risk factor for rapidly progressive interstitial lung disease in dermatomyositis. *Rheumatology (Oxford)* 2020; 59:1734–1742
64. Landon-Cardinal O, Koumako C, Hardouin G, et al. Severe axial and pelvi-femoral muscle damage in immune-mediated necrotizing myopathy evaluated by whole-body MRI. *Semin Arthritis Rheum* 2020; 50:1437–1440
65. Huang ZG, Gao BX, Chen H, et al. An efficacy analysis of whole-body magnetic resonance imaging in the diagnosis and follow-up of polymyositis and dermatomyositis. *PLoS One* 2017; 12:e0181069
66. Guerini H, Omoumi P, Guichoux F, et al. Fat suppression with Dixon techniques in musculoskeletal magnetic resonance imaging: a pictorial review. *Semin Musculoskelet Radiol* 2015; 19:335–347
67. Gómez-Andrés D, Dabaj I, Mompoint D, et al. Pediatric laminopathies: whole-body magnetic resonance imaging fingerprint and comparison with Sepn1 myopathy. *Muscle Nerve* 2016; 54:192–202
68. Capponi M, Pires Marafon D, Rivosecchi F, et al. Assessment of disease activity using a whole-body MRI derived radiological activity index in chronic nonbacterial osteomyelitis. *Pediatr Rheumatol Online J* 2021; 19:123
69. Leroy-Willig A, Willig TN, Henry-Feugeas MC, et al. Body composition determined with MR in patients with Duchenne muscular dystrophy, spinal muscular atrophy, and normal subjects. *Magn Reson Imaging* 1997; 15:737–744
70. Pichiecchio A, Uggetti C, Egitto MG, et al. Quantitative MR evaluation of body composition in patients with Duchenne muscular dystrophy. *Eur*

*Radiol* 2002; 12:2704–2709
71. Leung DG, Bocchieri AE, Ahlawat S, et al. Longitudinal functional and imaging outcome measures in FKRP limb-girdle muscular dystrophy. *BMC Neurol* 2020; 20:196
72. Krabbe S, Eshed I, Sørensen IJ, et al. Novel whole-body magnetic resonance imaging response and remission criteria document diminished inflammation during golimumab treatment in axial spondyloarthritis. *Rheumatology (Oxford)* 2020; 59:3358–3368
73. Song IH, Hermann K, Haibel H, et al. Effects of etanercept versus sulfasalazine in early axial spondyloarthritis on active inflammatory lesions as detected by whole-body MRI (ESTHER): a 48-week randomised controlled trial. *Ann Rheum Dis* 2011; 70:590–596
74. Althoff CE, Sieper J, Song IH, et al. Comparison of clinical examination versus whole-body magnetic resonance imaging of enthesitis in patients with early axial spondyloarthritis during 3 years of continuous etanercept treatment. *J Rheumatol* 2016; 43:618–624
75. Lecouvet FE, Vander Maren N, Collette L, et al. Whole body MRI in spondyloarthritis (SpA): preliminary results suggest that DWI outperforms STIR for lesion detection. *Eur Radiol* 2018; 28:4163–4173
76. Weckbach S, Schewe S, Michaely HJ, Steffinger D, Reiser MF, Glaser C. Whole-body MR imaging in psoriatic arthritis: additional value for therapeutic decision making. *Eur J Radiol* 2011; 77:149–155
77. Krabbe S, Østergaard M, Eshed I, et al. Whole-body magnetic resonance imaging in axial spondyloarthritis: reduction of sacroiliac, spinal, and entheseal inflammation in a placebo-controlled trial of adalimumab. *J Rheumatol* 2018; 45:621–629
78. Østergaard M, Eshed I, Althoff CE, et al. Whole-body magnetic resonance imaging in inflammatory arthritis: systematic literature review and first steps toward standardization and an OMERACT scoring system. *J Rheumatol* 2017; 44:1699–1705
79. Delgado J, Chauvin NA, Bedoya MA, Patel SJ, Anupindi SA. Whole-body magnetic resonance imaging in the evaluation of children with fever without a focus. *Pediatr Radiol* 2021; 51:605–613
80. Tavakoli AA, Reichert M, Blank T, et al. Findings in whole body MRI and conventional imaging in patients with fever of unknown origin-a retrospective study. *BMC Med Imaging* 2020; 20:94
81. Yokota S, Sakamoto K, Shimizu Y, et al. Evaluation of whole-body modalities for diagnosis of multifocal osteonecrosis—a pilot study. *Arthritis Res Ther* 2021; 23:83
82. Larbi A, Omoumi P, Pasoglou V, et al. Whole-body MRI to assess bone involvement in prostate cancer and multiple myeloma: comparison of the diagnostic accuracies of the T1, short tau inversion recovery (STIR), and high b-values diffusion-weighted imaging (DWI) sequences. *Eur Radiol* 2019; 29:4503–4513
83. Feldhaus JM, Garner HW, Wessell DE. Society of Skeletal Radiology member utilization and performance of whole-body MRI in adults. *Skeletal Radiol* 2020; 49:1731–1736
84. Chiabai O, Van Nieuwenhove S, Vekemans MC, et al. Whole-body MRI in oncology: can a single anatomic T2 Dixon sequence replace the combination of T1 and STIR sequences to detect skeletal metastasis and myeloma? *Eur Radiol* 2022
85. Danner A, Brumpt E, Alilet M, Tio G, Omoumi P, Aubry S. Improved contrast for myeloma focal lesions with T2-weighted Dixon images compared to T1-weighted images. *Diagn Interv Imaging* 2019; 100:513–519
86. Morone M, Bali MA, Tunariu N, et al. Whole-body MRI: current applications in oncology. *AJR* 2017; 209:[web]W336–W349
87. Summers P, Saia G, Colombo A, et al. Whole-body magnetic resonance imaging: technique, guidelines and key applications. *Ecancermedicalscience* 2021; 15:1164
88. Lecouvet FE, Pasoglou V, Van Nieuwenhove S, et al. Shortening the acquisition time of whole-body MRI: 3D T1 gradient echo Dixon vs fast spin echo for metastatic screening in prostate cancer. *Eur Radiol* 2020; 30:3083–3093
89. Herrmann J, Afat S, Brendlin A, Chaika M, Lingg A, Othman AE. Clinical evaluation of an abbreviated contrast-enhanced whole-body MRI for oncologic follow-up imaging. *Diagnostics (Basel)* 2021; 11:11
90. Taylor SA, Mallett S, Miles A, et al. Whole-body MRI compared with standard pathways for staging metastatic disease in lung and colorectal cancer: the Streamline diagnostic accuracy studies. *Health Technol Assess* 2019; 23:1–270
91. Tewattanarat N, Junhasavasdikul T, Panwar S, et al. Diagnostic accuracy of imaging approaches for early tumor detection in children with Li-Fraumeni syndrome. *Pediatr Radiol* 2022; 52:1283–1295
92. Schmidt CO, Sierocinski E, Baumeister S, Hegenscheid K, Völzke H, Chenot JF. Effects of whole-body MRI on outpatient health service costs: a general-population prospective cohort study in Mecklenburg-Vorpommern, Germany. *BMJ Open* 2022; 12:e056572
93. Gauthé M, Zarca K, Aveline C, et al. Comparison of $^{18}$F-sodium fluoride PET/CT, $^{18}$F-fluorocholine PET/CT and diffusion-weighted MRI for the detection of bone metastases in recurrent prostate cancer: a cost-effectiveness analysis in France. *BMC Med Imaging* 2020; 20:25
94. Kumasaka S, Motegi S, Kumasaka Y, Nishikata T, Otomo M, Tsushima Y. Whole-body magnetic resonance imaging (WB-MRI) with diffusion-weighted whole-body imaging with background body signal suppression (DWIBS) in prostate cancer: prevalence and clinical significance of incidental findings. *Br J Radiol* 2022; 95:20210459
95. Claeys KG, Goosens V. Whole-body muscle magnetic resonance imaging in patients with muscle symptoms: incidental findings and outcomes. *Eur J Neurol* 2021; 28:323–330
96. Basar Y, Alis D, Tekcan Sanli DE, Akbas T, Karaarslan E. Whole-body MRI for preventive health screening: management strategies and clinical implications. *Eur J Radiol* 2021; 137:109584
97. Donners R, Yiin RSZ, Koh DM, et al. Whole-body diffusion-weighted MRI in lymphoma: comparison of global apparent diffusion coefficient histogram parameters for differentiation of diseased nodes of lymphoma patients from normal lymph nodes of healthy individuals. *Quant Imaging Med Surg* 2021; 11:3549–3561
98. Tak CR, Biltaji E, Kohlmann W, et al. Cost-effectiveness of early cancer surveillance for patients with Li-Fraumeni syndrome. *Pediatr Blood Cancer* 2019; 66:e27629
99. North Carolina Industrial Commission website. CPT codes and fees: radiology 70010–79999. www.ic.nc.gov/ncic/pages/70000.htm. Accessed Apr 24, 2022
100. Schooler GR, Davis JT, Daldrup-Link HE, Frush DP. Current utilization and procedural practices in pediatric whole-body MRI. *Pediatr Radiol* 2018; 48:1101–1107